Revisiting log-periodic oscillations

Jean-Marc Luck

Revisiting log-periodic oscillations

Jean-Marc Luck

Université Paris-Saclay, CNRS, CEA, Institut de Physique Théorique,
91191 Gif-sur-Yvette, France

Abstract

This work is inspired by a recent study of a two-dimensional stochastic fragmentation model. We show that the configurational entropy of this model exhibits log-periodic oscillations as a function of the sample size, by exploiting an exact recursion relation for the numbers of its jammed configurations. This is seemingly the first statistical-mechanical model where log-periodic oscillations affect the size dependence of an extensive quantity. We then propose and investigate in great depth a one-dimensional analogue of the fragmentation model. This one-dimensional model possesses a critical point, separating a strong-coupling phase where the free energy is super-extensive from a weak-coupling one where the free energy is extensive and exhibits log-periodic oscillations. This model is generalized to a family of one-dimensional models with two integer parameters, which exhibit essentially the same phenomenology.

Keywords: Log-periodic oscillations, Oscillatory critical amplitudes, Fragmentation models, Finite-size scaling, Non-linear recursions, Discrete scale invariance

1. Introduction

From the very beginning of the renormalization-group era, it has been suggested that discrete real-space renormalization-group transformations might result in the modulation of critical behavior by a log-periodic function of the distance $t = |T - T_c|/T_c$ to the critical point [1, 2, 3]. Oscillatory critical amplitudes have been later observed and investigated for models defined on hierarchical lattices [4, 5, 6, 7, 8, 9, 10]. These lattices are self-similar geometric structures that exhibit discrete scale invariance, and therefore admit exact renormalization-group transformations. Similar features are shared by other fractal structures, on which various models have been shown to exhibit log-periodic oscillations (see e.g. [11, 12, 13, 14, 15, 16, 17]). The same phenomenon

Email address: jean-marc.luck@ipht.fr (Jean-Marc Luck)

has also been evidenced as a consequence of the fractal spectra of some aperiodic structures (see e.g. [18, 19, 20, 21]). The first ever mention of log-periodic oscillations seems to date back to 1948, long before the renormalization group was applied to phase transitions. In a work devoted to the theory of branching processes, Harris suggested that iterating a discrete mapping might yield log-periodic oscillations [22]. These oscillations have then been observed and studied in a more detailed investigation of a germane combinatorial problem, namely the enumeration of a class of binary trees [23].

Log-periodic oscillations have since then been reported in a broad variety of situations, as testified by the overview by Sornette [24]. In many settings including turbulence, fracture, earthquakes, financial crashes, and quantum gravity, the occurrence of oscillations is attributed to the emergence of an approximate discrete scale invariance. The associated scaling factor is often around two. Various physical mechanisms, including the period-doubling route to chaos, have been invoked to explain this phenomenon. In most of the above situations, the observed amplitude of oscillations is sizeable, i.e., of the order of 10 percent. This figure is in stark contrast with the historical example of critical phenomena, where log-periodic oscillations are typically tiny, with a magnitude of order 10^{-5}, and therefore hard to observe.

The singular behavior of physical quantities might also be modulated by periodic amplitudes for reasons that are unrelated to discrete scale invariance. Confining the discussion to statistical physics, one-dimensional disordered systems provide a breadth of examples of interest. There, periodic oscillations are eventually due to a discrete translation invariance, reflecting the atomic nature of the underlying lattice [25, 26]. In some models exhibiting anomalous biased diffusion, the growth law of the mean displacement is modulated by a log-periodic function of time [27, 28]. In electron and phonon spectra of disordered chains, the density of states has exponentially small Lifshitz tails, whose amplitudes are modulated by periodic functions of $(\Delta E)^{-1/2}$, where ΔE is the distance to the band edge [29, 30].

A last example, which motivated the present work, consists of a stochastic fragmentation model introduced in [31]. A rectangular sample with size (m, n) drawn on the square lattice is randomly cut into four smaller ones. The process is then repeated and stops when the system reaches a jammed configuration where all parts are sticks, i.e., the smaller size of each part equals unity. Consider for definiteness a square sample of size n. In the first step of the fragmentation process, the square is cut into four parts whose linear sizes are of the order of $n/2$. This observation suggests the emergence of some weak form of discrete scale invariance with scaling factor two, that is somehow reminiscent of what is claimed to occur in more complex phenomena such as turbulence or diffusion-limited aggregation [24]. The main advantage of the above fragmentation model, which triggered our interest, is the existence of an exact recursion formula for the numbers $Z_{m,n}$ of jammed configurations.

The setup of the present paper is as follows. In Section 2 we revisit the stochastic fragmentation model introduced in [31]. By exploiting the exact recursion recalled above, we demonstrate that the configurational entropy based

on the numbers $Z_{n,n}$ of jammed configurations on square samples exhibits tiny log-periodic oscillations in the sample size n. We then introduce and investigate in detail a one-dimensional (1D) toy model capturing the essential features of the combinatorics of the fragmentation model (Sections 3 to 6). In spite of its relative simplicity, the 1D model turns out to have a rich phenomenology, with a critical point (Section 4) separating a strong-coupling phase (Section 5) from a weak-coupling one (Section 6). In Section 7 we consider several other examples of 1D non-linear recursions. A brief discussion of our findings is given in Section 8.

2. The fragmentation model revisited

In this section we revisit the second fragmentation model introduced in [31]. This irreversible stochastic model is defined recursively as follows. The sample is a rectangle with size (m, n) drawn on the square lattice. The first step of the fragmentation consists in cutting the rectangle into four smaller ones, of respective sizes (i, j), $(i, n-j)$, $(m-i, j)$, $(m-i, n-j)$ (see Figure 1). The integers i and j are chosen uniformly in the ranges $1 \leq i \leq m-1$ and $1 \leq j \leq n-1$. The process is repeated and stops when the system reaches a jammed configuration where all parts are sticks, i.e., the smaller size of each part equals unity. Figure 2 shows a jammed tiling thus obtained on a square of size 50.

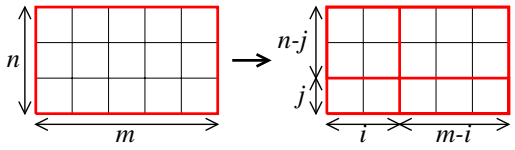

Figure 1: First step of the fragmentation of a rectangular sample with $m = 5$, $n = 3$, $i = 2$ and $j = 1$.

This fragmentation model enjoys the property that the stochastic histories of different rectangles are mutually independent from the epoch they are formed. As a consequence, the numbers $Z_{m,n}$ of jammed tiling configurations on rectangular samples of size (m, n) obey the recursion formula [31]

$$Z_{m,n} = \sum_{i=1}^{m-1} \sum_{j=1}^{n-1} Z_{i,j} Z_{i,n-j} Z_{m-i,j} Z_{m-i,n-j}, \tag{1}$$

with initial conditions $Z_{m,1} = Z_{1,n} = 1$ for all m and n. These 'initial' values actually express the 'final' condition that a jammed tiling is reached when all parts are sticks, i.e., the smaller size of each part equals unity. The recursion formula (1) determines all the numbers of jammed tilings, which obey the symmetry $Z_{m,n} = Z_{n,m}$. The first few of them are listed in Table 1.

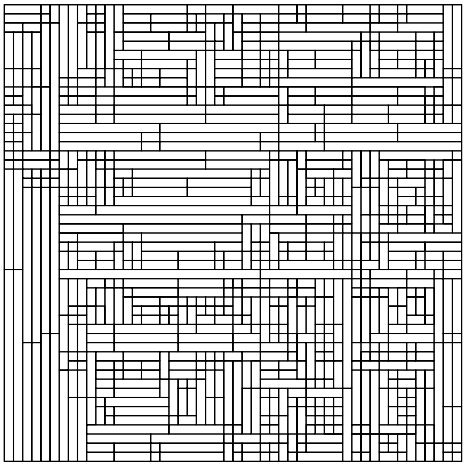

Figure 2: A jammed tiling of a square sample of size 50 (courtesy Paul Krapivsky).

$m \backslash n$	1	2	3	4	5	6	7	8
1	1	1	1	1	1	1	1	1
2	1	1	2	3	4	5	6	7
3	1	2	4	10	20	36	60	94
4	1	3	10	33	98	258	618	1 379
5	1	4	20	98	436	1 676	5 848	18 906
6	1	5	36	258	1 676	9 524	48 296	225 938
7	1	6	60	618	5 848	48 296	354 224	2 387 112
8	1	7	94	1 379	18 906	225 938	2 387 112	23 097 969

Table 1: Numbers $Z_{m,n}$ of jammed tilings on rectangular samples of size (m, n) for m and n up to 8.

The numbers $Z_{m,n}$ of tiling configurations grow very rapidly with the sample size (m, n). It is indeed to be expected that their logarithm is extensive, in the sense that it obeys an area law of the form

$$\ln Z_{m,n} \approx Smn, \tag{2}$$

where S is the bulk configurational entropy of the model per unit area [32, 33], for which the estimate $S \approx 0.2805$ is given in [31]. There are therefore some 10^{304} different configurations of jammed tilings on a square of size 50, only one of which is shown in Figure 2. A more complete thermodynamical expression for $\ln Z_{m,n}$, including the contributions S_e of the edges of the sample and S_c of

its corners, reads

$$\ln Z_{m,n} \approx Smn + 2S_e(m+n) + 4S_c. \tag{3}$$

The asymptotic behavior of $\ln Z_{m,n}$ emerges as a global property of the solution to the recursion (1), that has resisted all our attempts at analysis. As it turns out, the entropies S, S_e and S_c are modulated by log-periodic oscillations (see below). Moreover, at variance with the thermodynamical expectation (3), the edge and corner entropies S_e and S_c have a complex dependence on the aspect ratio $r = m/n$ of the sample (not described here). None of these peculiar features was mentioned in [31].

From now on, we focus our attention onto square samples. As already put forward in Section 1, a square of size n is cut into four parts whose sizes are of the order of $n/2$ in the first step of the fragmentation process. This suggests the emergence of some weak form of discrete scale invariance with scaling factor two, that is somehow reminiscent of what is claimed to occur in turbulence or in diffusion-limited aggregation [24]. This intuitive line of reasoning therefore opens the possibility that the area law (2) might be modulated by a 1-periodic oscillatory function of the variable

$$x = \frac{\ln n}{\ln 2}. \tag{4}$$

Our main goal is to demonstrate that log-periodic oscillations of this very kind are indeed present in the configurational entropy of the fragmentation model on square samples. To do so, we have devised an improved numerical scheme allowing an accurate iteration of the recursion (1) up to $n = 2^{10} = 1024$, where the integer $Z_{n,n}$ has some 127 000 digits, as $\ln Z_{n,n} \approx 294\,112.573\,480$. In order to avoid all overflows and underflows, we turn (1) into a recursion involving $\ln Z_{m,n}$, rather then $Z_{m,n}$ itself. This is possible because all terms entering (1) are positive, so that there can be no compensations. This goes as follows.

- For fixed m and n, find i_0 and j_0 corresponding to the largest term in the sum entering (1). This yields the estimate

$$\ln Z_{m,n} \approx \ln Z_{i_0,j_0} + \ln Z_{i_0,n-j_0} + \ln Z_{m-i_0,j_0} + \ln Z_{m-i_0,n-j_0}. \tag{5}$$

- Take all other terms into account by using the obvious identity

$$\ln(a+b) = \ln a + \ln(1+b/a), \tag{6}$$

  where $\ln a$ stands for the leading expression (5), whereas b stands for the sum of all other subleading terms with $(i,j) \neq (i_0,j_0)$.

For methodological reasons, we begin by considering the ratio

$$R_n = \frac{Z_{n,n}}{(Z_{n/2,n/2})^4} \tag{7}$$

for even n. The denominator of (7) is nothing but the central term in the expression (1) for $Z_{n,n}$, corresponding to $i = j = n/2$. It is therefore natural to interpret R_n as the effective number of terms contributing to the recursion (1) for $Z_{n,n}$.

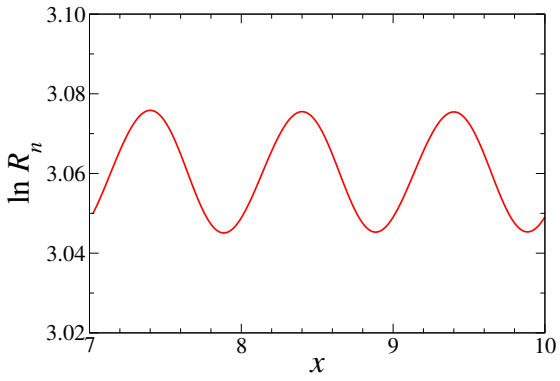

Figure 3: Logarithmic plot of the ratio R_n introduced in (7) against the logarithmic variable x defined in (4). The observed log-periodic oscillations imply that the edge configurational entropy S_e vanishes for square samples. The average value $(\ln R)_{\rm ave}$ gives access to the corner configurational entropy S_c (see (11)).

Figure 3 shows a logarithmic plot of R_n against the logarithmic variable x defined in (4). If the numbers $Z_{n,n}$ of tiling configurations were exactly given by the thermodynamic formula (3), we would have

$$\ln R_n \approx -4S_e n - 12S_c. \tag{8}$$

It is obvious from Figure 3 that the edge configurational entropy S_e vanishes for square samples. Indeed $\ln R_n$ would otherwise exhibit a linear growth in n with slope $4|S_e|$, i.e., an exponential growth in x.

The quantity $\ln R_n$ plotted in Figure 3 clearly exhibits 1-periodic oscillations in x. Here and throughout the following, we characterize an oscillatory periodic function $f(x)$ by its average $f_{\rm ave}$ over one period and by the relative magnitude of oscillations,

$$f_{\rm osc} = \frac{f_{\rm max} - f_{\rm min}}{f_{\rm ave}}. \tag{9}$$

The data shown in Figure 3 yield

$$(\ln R)_{\rm ave} \approx 3.060, \qquad (\ln R)_{\rm osc} \approx 9.8\ 10^{-3}. \tag{10}$$

Pre-asymptotic corrections to log-periodic behavior are negligible in the range shown in Figure 3.

The corner configurational entropy of a large square can be estimated as

$$S_c = -\frac{(\ln R)_{\rm ave}}{12} \approx -0.255, \tag{11}$$

whereas the effective number R_n of terms entering the recursion (1) approaches the rather large but finite limit

$$R_{\rm eff} = \exp\left((\ln R)_{\rm ave}\right) \approx 21.32. \tag{12}$$

A more accurate definition of the bulk configurational entropy of square samples is given by

$$S_n = \frac{\ln Z_{n,n} - 4S_c}{n^2}, \tag{13}$$

where S_c is taken from (11). Figure 4 shows that this quantity exhibits very small but very clear 1-periodic oscillations in the logarithmic variable x. This is seemingly the first instance where log-periodic oscillations are reported for the size dependence of an extensive quantity in a statistical-mechanical model.

The subtraction of the corner entropy $4S_c$ has drastically improved convergence, so that corrections are again negligible in the range shown in Figure 4. From a quantitative viewpoint, we have

$$S_{\rm ave} \approx 0.280481, \qquad S_{\rm osc} \approx 1.44\ 10^{-4}. \tag{14}$$

The numerical value of $S_{\rm ave}$ is in full agreement with the estimate $S \approx 0.2805$ given in [31]. The magnitude $S_{\rm osc}$ of oscillations is within the range commonly observed, e.g. in the critical properties of models on hierarchical lattices.

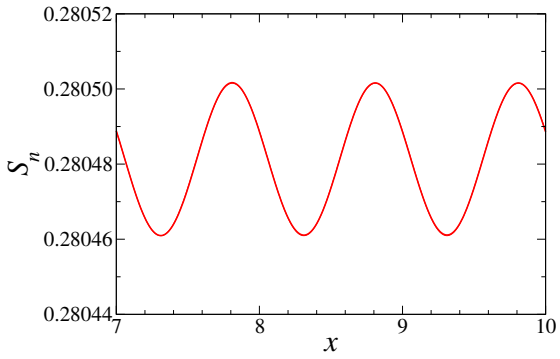

Figure 4: Configurational entropy S_n defined in (13), plotted against the logarithmic variable x defined in (4). This quantity exhibits very small 1-periodic oscillations (see (14)).

3. 1D model: generalities

In this section we introduce a one-dimensional (1D) analogue of the combinatorics of jammed configurations in the fragmentation model investigated in Section 2. This 1D toy model captures the main features of the fragmentation model, whereas it is simple enough to be studied in great depth (see Sections 4

to 6). Furthermore, the 1D model has a richer phenomenology than the original fragmentation model, with a critical point separating a weak-coupling phase, where the free energy is extensive and exhibits oscillations, from a strong-coupling one, where the free energy is super-extensive and does not manifest oscillations.

The 1D model is defined by the recursion relation

$$Z_n = \sum_{k=1}^{n-1} Z_k^2 Z_{n-k}^2 \qquad (n \geq 2). \tag{15}$$

This recursion keeps the essential characteristics of its two-dimensional analogue (1), including chiefly the global degree four of the right-hand side, and the symmetric roles of Z_k and Z_{n-k}. The recursion (15) requires only one initial condition, namely Z_1. We set

$$Z_1 = a. \tag{16}$$

Hereafter the parameter a is chosen to be positive, and viewed as a coupling constant. The Z_n are then positive, and interpreted as partition functions.

The simplest of all initial conditions, $a = 1$, yields integer values for the Z_n:

$$\begin{aligned} &Z_1 = 1, \qquad Z_2 = 1, \qquad Z_3 = 2, \qquad Z_4 = 9, \qquad Z_5 = 170, \\ &Z_6 = 57\,978, \qquad Z_7 = 6\,722\,955\,416, \end{aligned} \tag{17}$$

and so on. These numbers are listed as sequence number A053294 in the OEIS [34], where they are defined as the solution to the very recursion (15), without any motivation nor any useful result.

For a generic initial condition, we have

$$\begin{aligned} Z_2 &= a^4, \\ Z_3 &= 2a^{10}, \\ Z_4 &= a^{16} + 8a^{22}, \\ Z_5 &= 8a^{28} + 2a^{34} + 32a^{40} + 128a^{46}, \\ Z_6 &= 18a^{40} + 32a^{46} + 128a^{52} + 128a^{58} + 64a^{64} + 1032a^{70} \\ &\quad + 4352a^{76} + 3072a^{82} + 16384a^{88} + 32768a^{94}, \end{aligned} \tag{18}$$

and so on. The partition function Z_n is a polynomial in a of the form

$$Z_n = A_n a^{\alpha_n} + \cdots + B_n a^{\beta_n}. \tag{19}$$

The terms $A_n a^{\alpha_n}$ of lowest degrees and $B_n a^{\beta_n}$ of largest degrees will be investigated in detail hereafter (see (38), (39), (51), (63)). Furthermore, the degrees of successive powers of a differ by six, and so

$$Z_n = a^{\alpha_n}\, P_n(z), \tag{20}$$

where

$$P_n(z) = A_n + \cdots + B_n z^{\Delta_n} \tag{21}$$

is a polynomial in the variable

$$z = a^6 \tag{22}$$

with degree

$$\Delta_n = \frac{\beta_n - \alpha_n}{6}. \tag{23}$$

We have

$$\begin{aligned}
P_1(z) &= 1, \\
P_2(z) &= 1, \\
P_3(z) &= 2, \\
P_4(z) &= 1 + 8z, \\
P_5(z) &= 8 + 2z + 32z^2 + 128z^3, \\
P_6(z) &= 18 + 32z + 128z^2 + 128z^3 + 64z^4 + 1032z^5 \\
&\quad + 4352z^6 + 3072z^7 + 16384z^8 + 32768z^9,
\end{aligned} \tag{24}$$

and so on. Table 2 gives the degrees α_n, β_n and Δ_n up to $n = 14$.

n	α_n	β_n	Δ_n	n	α_n	β_n	Δ_n
1	1	1	0	8	64	382	53
2	4	4	0	9	88	766	113
3	10	10	0	10	112	1534	237
4	16	22	1	11	136	3070	489
5	28	46	3	12	160	6142	997
6	40	94	9	13	184	12286	2017
7	52	190	23	14	208	24574	4061

Table 2: Degrees α_n, β_n and Δ_n, defined in (19) and (23), up to $n = 14$.

Figure 5 shows a plot of the 237 zeros (or roots) of the polynomial $P_{10}(z)$ in the complex z-plane. Most zeros sit near the circle with radius $R = 1/2$, shown in black (see (43)). The zeros pinch the positive real axis at $z_c \approx 0.411$ (red symbol), corresponding to $a_c \approx 0.862$. This observation points toward the emergence of a non-trivial phase diagram driven by the initial condition (16), where a critical point at a_c separates a strong-coupling phase ($a > a_c$) from a weak-coupling one ($a < a_c$). The detailed analysis performed in Sections 4 to 6 corroborates this picture.

4. 1D model: critical region

The 1D model has a critical point at the following value

$$a_c = 0.862\,322\,847\,096\,001\,235\,198\,066\ldots \tag{25}$$

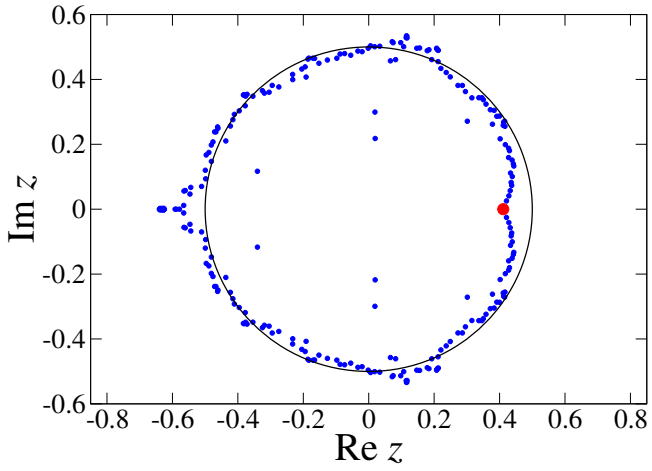

Figure 5: Blue symbols: the 237 zeros of the polynomial $P_{10}(z)$ in the complex z-plane. Red symbol: accumulation point of the zeros on the positive real axis at $z_c \approx 0.411$. The radius $R = 1/2$ of the black circle is the modulus of a typical zero of $P_n(z)$ for large n (see (43)).

of the coupling constant. This critical point is somewhat similar to a separatrix in nonlinear dynamics. The accuracy of the above number will be commented on at the end of this section.

Right at $a = a_c$, the partition functions obey a power law of the form

$$Z_n \approx C\, n^{\gamma}. \tag{26}$$

Inserting this asymptotic behavior into (15), and using a continuum setting where the sum over k is replaced by an integral over $y = k/n$, we successively obtain $\gamma = 4\gamma + 1$, hence

$$\gamma = -\frac{1}{3}, \tag{27}$$

and

$$C = C^4 \int_0^1 (y(1-y))^{-2/3} \mathrm{d}y, \tag{28}$$

hence

$$C = \left(\frac{\Gamma(2/3)}{\Gamma^2(1/3)} \right)^{1/3} = 0.573\,557\,545\ldots \tag{29}$$

Near $a = a_c$, along the lines of finite-size scaling theory [35, 36], we expect a scaling behavior of the form

$$Z_n \approx C\, n^{-1/3} \big(1 + D(a - a_c) n^{\sigma} + \cdots \big), \tag{30}$$

where the crossover exponent

$$\sigma = \frac{1}{\nu} \tag{31}$$

is the inverse of the correlation length exponent ν. Inserting the scaling behavior (30) into (15), working to first order in $a - a_c$, and using the same continuum setting as above, we obtain the following 'quantization condition' for the crossover exponent:

$$\frac{\Gamma(\sigma + 1/3)\Gamma(2/3)}{\Gamma(\sigma + 2/3)\Gamma(1/3)} = \frac{1}{4}, \tag{32}$$

hence

$$\sigma = 8.260\,875\,323\ldots, \quad \nu = 0.121\,052\,547\ldots \tag{33}$$

The above scaling analysis yields the exact values of γ, C, σ and ν, but it neither predicts a_c nor the crossover amplitude D.

As a consequence of the very large crossover exponent σ, the recursion (15) is very unstable in the vicinity of a_c, i.e., very sensitive to deviations from a_c, so that the very accurate numerical value of a_c given in (25) can be obtained. This level of accuracy will be needed at some places hereafter.

5. 1D model: strong-coupling phase

In this section we consider the strong-coupling phase ($a > a_c$) of the 1D model, which is simpler to analyze than its weak-coupling partner.

The partition functions Z_n grow very fast in this phase, so that the sum in (15) is expected to be dominated by its extremal terms ($k = 1$ and $k = n-1$). Forgetting about prefactors, this reads

$$Z_n \sim Z_{n-1}^2. \tag{34}$$

Several heuristic equations of this kind will be met hereafter in the context of 1D models. The recursion (34) does not point toward the existence of oscillations. It yields an exponentially super-extensive growth law of the form

$$\ln Z_n \approx K(a)\, 2^n. \tag{35}$$

The quantity $K(a)$ is referred to as the generalized free energy of the model in its strong-coupling phase.

5.1. $a \to \infty$ regime

Let us begin by considering the situation where $a \to \infty$. In this regime, we have (see (19))

$$Z_n \approx B_n a^{\beta_n}. \tag{36}$$

The above assumption that the sum in (15) is dominated by its two extremal terms is consistent and translates to the recursion relations

$$\beta_n = 2(\beta_{n-1} + 1), \qquad B_n = 2B_{n-1}^2 \qquad (n \geq 3), \tag{37}$$

yielding

$$\beta_n = 3\,2^{n-1} - 2 \qquad (n \geq 1) \tag{38}$$

and

$$B_n = 2^{2^{n-2}-1} \qquad (n \geq 2). \tag{39}$$

These results agree with the form (35) and yield the asymptotic form of $K(a)$ at large a, namely

$$K_{\rm asy}(a) = \frac{3}{2} \ln a + \frac{1}{4} \ln 2. \tag{40}$$

The first correction term to the above asymptotic form is in $1/a^6$. The expression (40) vanishes at

$$a_0 = 2^{-1/6} = 0.890\,898\,718\ldots, \tag{41}$$

whereas $K(a)$ vanishes at a_c (see (25)). The small difference (3 percent) between a_c and its strong-coupling approximation a_0 will be demonstrated in Figure 6. It can be alternatively illustrated in terms of the zeros of the polynomials $P_n(z)$, shown in Figure 5 for $n = 10$. The form (21) implies that the product of all zeros z_k of $P_n(z)$ reads

$$\prod_{k=1}^{\Delta_n} z_k = (-1)^{\Delta_n} \frac{A_n}{B_n}. \tag{42}$$

It will be shown below (see (51) and (63)) that α_n and A_n grow much less rapidly than β_n and B_n. As a consequence, we have $\Delta_n \approx \beta_n/6 \approx 2^{n-2}$ and

$$R = \lim_{n\to\infty} \left(\frac{A_n}{B_n} \right)^{1/\Delta_n} = \frac{1}{2}. \tag{43}$$

This number represents the modulus $|z_k|$ of a typical zero of $P_n(z)$ for large n. It is therefore to be expected that most zeros lie near the circle with radius $1/2$. This prediction is corroborated by Figure 5. Finally, $z_0 = a_0^6 = 1/2$ sits right on the above circle, whereas $z_c = a_c^6$, shown by a red symbol in Figure 5, is slightly inside that circle.

5.2. Generic values ($a > a_c$)

We have performed a numerical iteration of the recursion (15) by means of the scheme already used in Section 2 (see (5) and (6)). This numerical analysis clearly demonstrates that the super-exponential behavior (35) holds throughout the strong-coupling phase. Figure 6 shows the generalized free energy $K(a)$ thus obtained and its asymptotic form $K_{\rm asy}(a)$, plotted against a in some range above the critical point. The values a_c and a_0 where these functions vanish are shown by arrows. The relatively small difference between these numbers, emphasized just above, goes hand in hand with the observation that $K_{\rm asy}(a)$ provides a good overall representation of the true $K(a)$, except in the immediate vicinity of the critical point.

The critical behavior of the generalized free energy $K(a)$ can be predicted by means of the following scaling argument. If $a - a_c$ is very small, the exponential

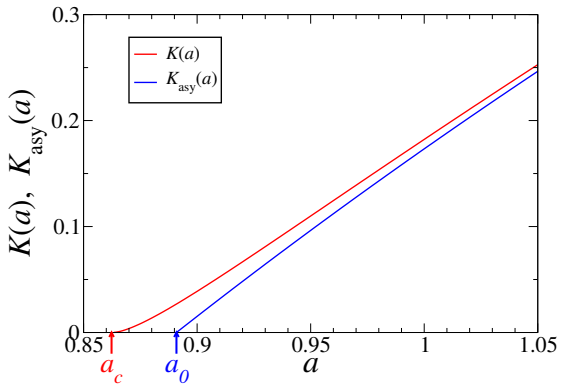

Figure 6: Generalized free energy $K(a)$ (red) and its asymptotic form $K_{\rm asy}(a)$ (blue), plotted against a in some range above the critical point. Arrows: values a_c and a_0 where these functions respectively vanish. The asymptotic form $K_{\rm asy}(a)$ provides a good representation of $K(a)$, except in the vicinity of the critical point.

growth (35) only sets in when the sample size n has exceeded a crossover length diverging as $(a - a_c)^{-\nu}$. This yields an exponentially small essential critical singularity of the form

$$K(a) \sim \exp\left(-C_1(a - a_c)^{-\nu}\right). \tag{44}$$

This functional form is corroborated by Figure 7, showing $-\ln K(a)$ against $(a - a_c)^{-\nu}$. The slope of the blue line yields

$$C_1 \approx 9.3. \tag{45}$$

The rightmost plotted point is the deepest into the critical region, with $a - a_c \approx 2.05\ 10^{-15}$ and $K(a) \sim 10^{-233}$. These numbers call for two remarks. First, only the numerical evaluation of exact equations such as the recursion (15) can achieve such accuracy. Second, it is crucial to use a very accurate value of a_c itself (see (25)).

6. 1D model: weak-coupling phase

We now turn to the weak-coupling phase of the 1D model ($a < a_c$). There, it will be shown that the free energy is extensive, growing as n^2, and exhibits log-periodic oscillations as a function of the sample size n, corresponding to a discrete scaling factor two, just as the two-dimensional fragmentation model studied in Section 2.

The partition functions Z_n fall off to zero as n increases, so that the sum in (15) is expected to be dominated by its central terms ($k \approx n/2$). Forgetting about prefactors, this reads

$$Z_n \sim Z_{n/2}^4. \tag{46}$$

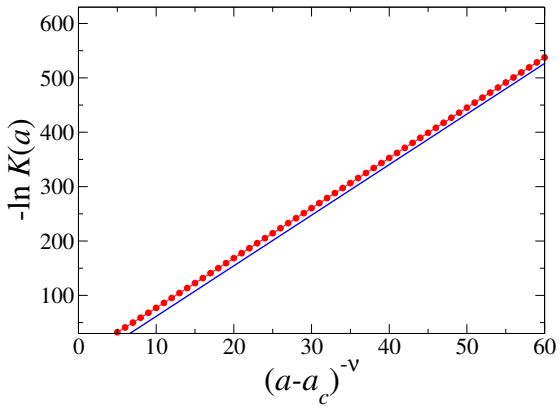

Figure 7: Plot of $-\ln K(a)$ against $(a-a_c)^{-\nu}$, corroborating the critical singularity (44) of the generalized free energy. The slope of the blue line yields $C_1 \approx 9.3$. The rightmost point is the deepest into the critical region, with $a - a_c \approx 2.05\ 10^{-15}$ and $K(a) \sim 10^{-233}$.

This heuristic relation suggests a growth of $\ln Z_n$ of the form

$$\ln Z_n \approx -F(a,x)\, n^2, \tag{47}$$

where $F(a,x)$ exhibits 1-periodic oscillations in the logarithmic variable x defined in (4). This quantity is hereafter referred to as the free energy (density) of the model.

6.1. $a \to 0$ regime

Let us begin by considering the situation where $a \to 0$. In this regime, the presence of log-periodic oscillations can be explained in simple terms. We have (see (19))

$$Z_n \approx A_n a^{\alpha_n}. \tag{48}$$

We shall successively investigate the degrees α_n and the coefficients A_n.

The degrees α_n entering (48) obey the recursion

$$\alpha_n = 2 \min_{1\le k\le n-1} (\alpha_k + \alpha_{n-k}). \tag{49}$$

These integers are given in Table 2 up to $n = 12$. They are listed as sequence number A073121 in the OEIS [34], together with useful formulas and references. In particular, they obey the recursions

$$\alpha_{2n} = 4\alpha_n, \qquad \alpha_{2n+1} = 2(\alpha_n + \alpha_{n+1}). \tag{50}$$

These relations exhibit a discrete scale invariance with scaling factor two. In particular, $\alpha_n = n^2$ whenever $n = 2^m$ is a power of two. For n in the interval $2^m \le n \le 2^{m+1}$, the degrees α_n exhibit an exact linear growth in n, of the form

$$\alpha_n = 2^m(3n - 2^{m+1}), \tag{51}$$

so that

$$\alpha_n - n^2 = (2^{m+1} - n)(n - 2^m). \tag{52}$$

It is then useful to split the logarithmic variable x defined in (4) into its integer and fractional parts according to

$$x = \frac{\ln n}{\ln 2} = m + \xi \qquad (0 \le \xi \le 1), \tag{53}$$

and to introduce another reduced co-ordinate,

$$\eta = \frac{n}{2^m} - 1 = 2^\xi - 1, \tag{54}$$

that is also in the range $0 \le \eta \le 1$. The result (51) can be exactly recast as

$$\alpha_n = n^2 f(x), \tag{55}$$

where $f(x)$ is a 1-periodic function of x, given by

$$f(x) = 2^{-\xi}(3 - 2^{1-\xi}) = 1 + \frac{\eta(1-\eta)}{(1+\eta)^2} \tag{56}$$

in terms of the co-ordinates ξ or η. The function $f(x)$ will be plotted in Figure 8. It reaches its minimum $f_{\min} = 1$ at integer x and its maximum $f_{\max} = 9/8$ for $\xi = \ln(4/3)/\ln 2$, i.e., $\eta = 1/3$. We have

$$f_{\rm ave} = \frac{3}{4\ln 2} = 1.082\,021\,280\ldots, \qquad f_{\rm osc} = \frac{\ln 2}{6} = 0.115\,524\,530\ldots \tag{57}$$

We have thus established the validity of the scaling form (47), including log-periodic oscillations, to leading order as $a \to 0$, and derived a first estimate of the free energy in the small-a regime,

$$F(a,x) \approx f(x)|\ln a|. \tag{58}$$

Let us now turn to the analysis of the coefficients A_n entering (48). The minimum in (49) turns out to be generically highly degenerate. More precisely, for n in the interval $2^m \le n \le 2^{m+1}$, i.e., $n = 2^m + i$ with $0 \le i \le 2^m$, this minimum is reached for all integers k of the form $k = 2^{m-1} + j$, where j runs over the following range:

$$\begin{cases} 0 \le i \le 2^{m-1} : & 0 \le j \le i, \\ 2^{m-1} \le i \le 2^m : & i - 2^{m-1} \le j \le 2^{m-1}. \end{cases} \tag{59}$$

Denoting by K_n the set of integers k defined above, the coefficients A_n obey the recursion

$$A_n = \sum_{k \in K_n} A_k^2 A_{n-k}^2. \tag{60}$$

When $n = 2^m$ is a power of two, the set K_n consists of a single element, $k = n/2$, and so $A_n = 1$. When $n = 3\,2^{m-1}$ is half-way between two successive powers of

two, the set K_n is the largest, with $2^{m-1}+1$ elements, and the coefficient A_n is (locally) maximal. We have

$$A_3 = 2, \quad A_6 = 18, \quad A_{12} = 113\,170, \tag{61}$$

and so on. More generally, we have the symmetry

$$A_n = A_{\tilde{n}}, \qquad \tilde{n} = 3\,2^m - n. \tag{62}$$

The coefficients A_n obey the asymptotic growth law

$$\ln A_n \approx n^2 g(x), \tag{63}$$

where $g(x)$ is a 1-periodic function of x. We have thus obtained a more complete estimate of the free energy in the small-a regime:

$$F(a,x) \approx f(x)|\ln a| - g(x). \tag{64}$$

The function $g(x)$ is positive, vanishes at integer x, and its average reads

$$g_{\rm ave} \approx 0.058\,187\,830. \tag{65}$$

At variance with (49), the recursion (60) cannot be solved in closed form, so that no analytic expression for $g(x)$ is available. As a consequence of (59), $g(x)$ exhibits cusps at (presumably) all dyadic values $\eta = j/2^k$ of the coordinate η introduced in (54). The strongest of these cusps are situated at $\eta = 2^{-k}$ and $\eta = 1 - 2^{-k}$. Figure 8 shows the 1-periodic functions $f(x) - 1$ and $g(x)$ over one period. The cusp singularities of $g(x)$ are not visible at this scale. Figure 9 shows the ratio

$$R(x) = \frac{g(x)}{f(x) - 1} \tag{66}$$

against the co-ordinate η introduced in (54). The formulas (52) and (62) imply that $R(x)$ is invariant under the change of η into $1 - \eta$. The two main series of cusp singularities are now clearly visible (red symbols).

6.2. Generic values ($a < a_c$)

A numerical iteration of the recursion (15) by means of the scheme already used in Section 2 (see (5) and (6)) clearly demonstrates that the scaling behavior (47) holds throughout the weak-coupling phase. We shall focus our attention onto the average $F_{\rm ave}(a)$ and the relative magnitude of oscillations $F_{\rm osc}(a)$ of the free energy $F(a,x)$.

In the $a \to 0$ regime, the estimate (64) shows that the average free energy diverges logarithmically according to

$$F_{\rm ave}(a) \approx f_{\rm ave}|\ln a| - g_{\rm ave}, \tag{67}$$

where $f_{\rm ave}$ and $g_{\rm ave}$ are respectively given in (57) and (65), whereas $F_{\rm osc}(a)$ goes to the finite limit (see (57))

$$F_{\rm osc}(0) = f_{\rm osc} = 0.115\,524\,530\ldots, \tag{68}$$

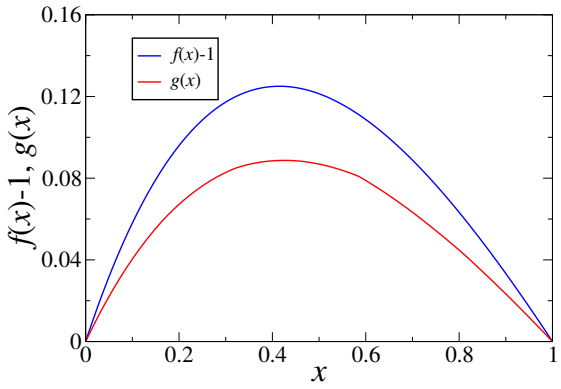

Figure 8: The 1-periodic functions $f(x) - 1$ (blue) and $g(x)$ (red), entering the full estimate (64) of the free energy in the small-a regime, plotted against x over one period.

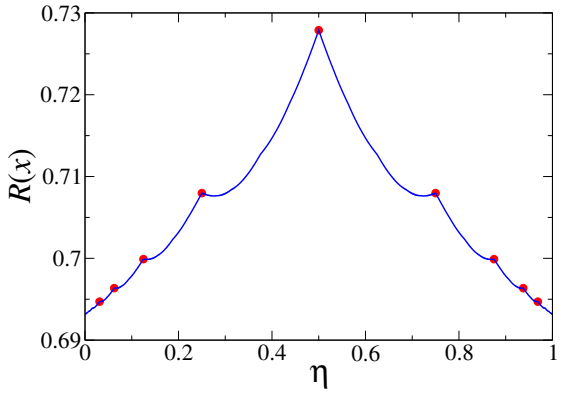

Figure 9: Ratio $R(x)$ defined in (66), plotted against the co-ordinate η. Equations (52) and (62) imply that $R(x)$ is invariant under the change of η into $1 - \eta$. Red symbols: two main series of cusps at $\eta = 2^{-k}$ and $\eta = 1 - 2^{-k}$.

whose value is quite sizeable.

In the critical regime ($a \to a_c$), scaling theory suggests that the average free energy vanishes according to

$$F_{\rm ave}(a) \approx C_2(a_c - a)^{2\nu}, \tag{69}$$

whereas the relative magnitude of oscillations has a finite limit $F_{\rm osc}(a_c)$. These expectations are corroborated by Figures 10 and 11. The data plotted there have been extrapolated by means of very accurate 4th-degree polynomial fits. There is no rationale behind the choice of the abscissas used in these plots: the chosen powers of $a_c - a$ just turn out to allow for accurate extrapolations.

Figure 10 shows the combination $(a_c - a)^{-2\nu} F_{\rm ave}(a)$ against $(a_c - a)^{\nu}$, yielding

$$C_2 \approx 0.0050. \tag{70}$$

Comparing this number to the amplitude C_1 given in (45), we notice that, even though C_1 is large and C_2 is small, the dimensionless combination $C_1^2 C_2 \approx 0.43$ is of order unity. Figure 11 shows $F_{\rm osc}(a)$ against $(a_c - a)^{2\nu}$, yielding

$$F_{\rm osc}(a_c) \approx 0.00111. \tag{71}$$

The relative magnitude of free energy oscillations at the critical point is therefore very small, but definitely non zero.

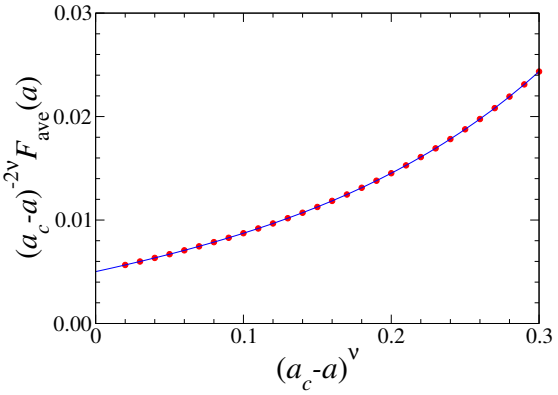

Figure 10: Red symbols: $(a_c - a)^{-2\nu} F_{\rm ave}(a)$ against $(a_c - a)^{\nu}$. Blue curve: polynomial fit yielding $C_2 \approx 0.0050$. The individual amplitudes C_1 and C_2 entering (44) and (69) are respectively large and very small, but their dimensionless combination $C_1^2 C_2 \approx 0.43$ is of order unity.

As the coupling constant a is increased from 0 to a_c, the average free energy $F_{\rm ave}(a)$ decreases steadily from infinity to zero, interpolating smoothly between the behaviors (67) and (69). In the same time, the relative magnitude $F_{\rm osc}(a)$ of oscillations decreases by a factor of order 100 from (68) to (71). Figure 12 shows that $F_{\rm osc}(a)$ does not decay monotonically between those two limits. In particular, it exhibits a cusp at $a_* = 0.537\,750\ldots$

The cusp in Figure 12 has to do with a change in the shape of the 1-periodic function $F(a, x)$. Figure 13 shows the reduced oscillations $F(a, x)/F_{\rm ave}(a)$ against the logarithmic variable x. Two consecutive periods are shown for clarity. For the smaller values of a (upper panel), the oscillations strongly decrease in magnitude, while keeping essentially the shape of $f(x)$ (see Figure 8), with a cusp around a single minimum at integer x. For a near a_* (lower panel), the structure of the oscillations becomes richer and changes rapidly with a. A second minimum with a cusp develops at $\eta = 1/2$, i.e., $\xi = \ln(3/2)/\ln 2 = 0.584\,962\ldots$ This second cusp and the original one have exactly the same height at $a = a_*$. This degeneracy causes the structure observed in Figure 12. For larger a (not shown), the oscillations soon become very small and harmonic.

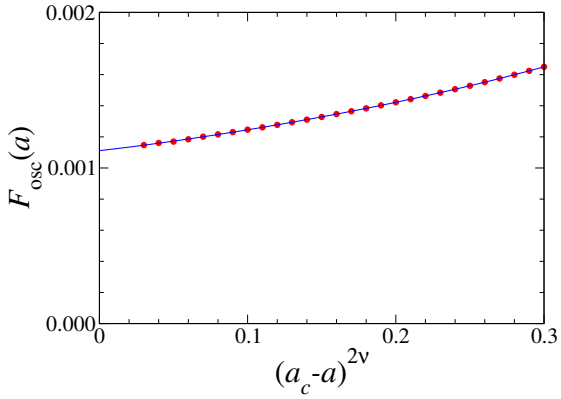

Figure 11: Red symbols: $F_{\rm osc}(a)$ against $(a_c-a)^{2\nu}$. Blue curve: polynomial fit yielding $F_{\rm osc}(a_c) \approx 0.00111$. The relative magnitude of free energy oscillations at the critical point is therefore very small, but definitely non zero.

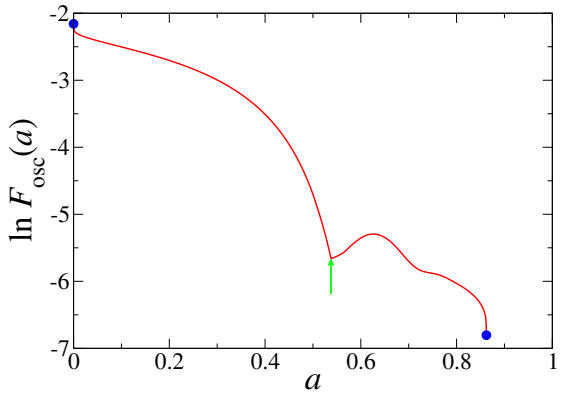

Figure 12: Logarithmic plot of $F_{\rm osc}(a)$ against a all over the weak-coupling phase. Blue symbols: limit values (68) at $a=0$ and (71) at $a=a_c$. Green arrow: cusp in $F_{\rm osc}(a)$ due to the change in the shape of the 1-periodic function $F(a,x)$ at $a_* \approx 0.537750$.

7. Further 1D examples

In this section we propose four other 1D analogues of the recursion (15) for the partition functions of the fragmentation model. In each case, we determine whether the model may cross a phase transition when its initial conditions are varied and whether is exhibits log-periodic oscillations in one of its phases. These outcomes lead us to introduce, as our fifth example, what we can think of as the most general recursion of this kind exhibiting log-periodic oscillations.

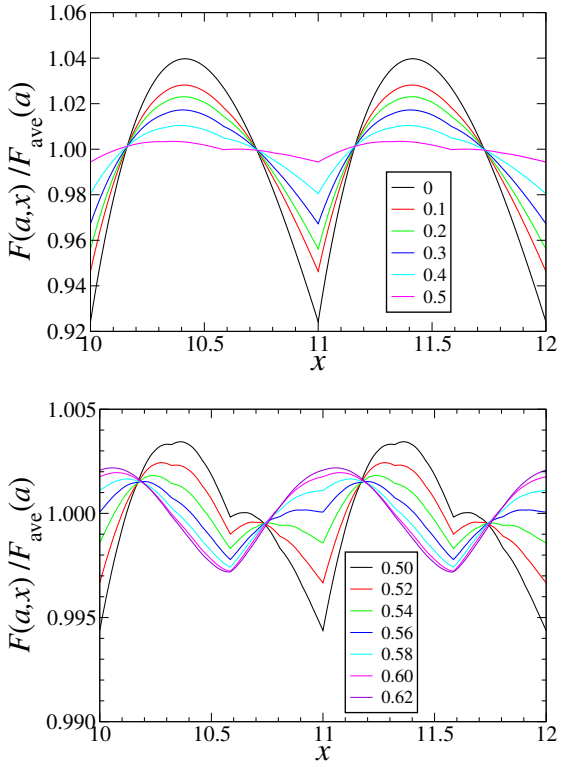

Figure 13: Reduced oscillations $F(a,x)/F_{\rm ave}(a)$, plotted against the logarithmic variable x for several a (see legends). Note the different vertical scales in both panels.

Example 1

This first example is obtained by suppressing the squares in the recursion (15) defining the 1D model. We thus obtain the bilinear recursion

$$Z_n = \sum_{k=1}^{n-1} Z_k Z_{n-k} \qquad (n \geq 2), \tag{72}$$

with initial condition $Z_1 = a$. In terms of the generating series

$$G(z) = \sum_{n\geq 1} Z_n z^n, \tag{73}$$

this reads

$$G(z) = az + G(z)^2, \tag{74}$$

hence

$$G(z) = \frac{1-\sqrt{1-4az}}{2}. \tag{75}$$

The partition functions therefore read

$$Z_n = C_{n-1} a^n \approx \frac{(4a)^n}{4\sqrt{\pi n^3}}, \tag{76}$$

where

$$C_{n-1} = \frac{(2n-2)!}{n!(n-1)!} \tag{77}$$

is the $(n-1)$-st Catalan number. These integers have a panoply of combinatorial interpretations. They are listed as sequence number A000108 in the OEIS [34], together with many useful formulas and references. The exponential growth rate of the Z_n depends smoothly on the initial condition. This example neither exhibits a phase transition nor oscillations.

Example 2

This second example is an extension of the previous one, defined by the trilinear recursion

$$Z_n = \sum_{k+l+m=n} Z_k Z_l Z_m \qquad (n \geq 3), \tag{78}$$

with initial conditions $Z_1 = a$ and $Z_2 = b$. For $a = b = 1$, the Z_n are positive integers which count ternary trees. They are listed as sequence number A019497 in the OEIS [34]. In full generality, the corresponding generating series, defined in analogy with (73), obeys

$$G(z) = az + bz^2 + G(z)^3. \tag{79}$$

We thus obtain the asymptotic behavior

$$Z_n \approx \frac{C}{n^{3/2}\, {z_0}^n}, \tag{80}$$

where z_0 is the smallest zero of the discriminant of (79), namely

$$\Delta = 27z^2(a+bz)^2 - 4. \tag{81}$$

In the range of physical relevance (a and b positive), the exponential growth rate $1/z_0$ is positive and has a smooth dependence on the initial conditions. This example therefore neither exhibits a phase transition nor oscillations.

Example 3

The third example is obtained by replacing each square in (15) by a higher power, namely

$$Z_n = \sum_{k=1}^{n-1} Z_k^p Z_{n-k}^p \qquad (n \geq 2), \tag{82}$$

with $Z_1 = a$. For any integer $p \geq 3$, the model exhibits the very same phenomenology as the 1D model investigated above, with a critical point at some p-dependent a_c. The strong-coupling phase ($a > a_c$) is captured by the heuristic equation

$$Z_n \sim Z_{n-1}^p, \tag{83}$$

generalizing (34) and yielding an exponentially growing free energy of the form

$$\ln Z_n \approx K(a)\, p^n. \tag{84}$$

The weak-coupling phase ($a < a_c$) is captured by the heuristic equation

$$Z_n \sim Z_{n/2}^{2p}, \tag{85}$$

generalizing (46) and yielding a free energy growing as

$$\ln Z_n \approx -F(a,x)\, n^d, \tag{86}$$

where the effective dimension reads

$$d = \frac{\ln 2p}{\ln 2}, \tag{87}$$

and $F(a,x)$ is a 1-periodic function of the logarithmic variable x defined in (4).

Example 4

The fourth example is obtained by replacing the squares in (15) by two different integer powers p and q, such that $p > q \geq 1$, namely

$$Z_n = \sum_{k=1}^{n-1} Z_k^p Z_{n-k}^q \qquad (n \geq 2), \tag{88}$$

with $Z_1 = a$. This is the first situation where Z_k and Z_{n-k} play asymmetrical roles. The model has a critical point at some a_c depending on p and q. The strong-coupling phase ($a > a_c$) is similar to that of the previous example. In the weak-coupling phase ($a < a_c$), the free energy grows as a power of the sample size, namely

$$\ln Z_n \approx -F(a)\, n^d, \tag{89}$$

where the effective dimension d is given by

$$\left(p^{1/(d-1)} - 1\right)\left(q^{1/(d-1)} - 1\right) = 1. \tag{90}$$

The power-law (89) is modulated by slowly damped erratic oscillations. This example therefore exhibits a continuous phase transition, but no everlasting log-periodic oscillations.

Example 5

This fifth example is meant to represent the most general recursion exhibiting log-periodic oscillations, at least within the class of models under scrutiny. The study of the previous examples suggests that the following ingredients are necessary: each partition function enters non-linearly and all parts play symmetric roles. We are thus led to consider the recursion

$$Z_n = \sum_{k_1+\cdots+k_r=n} Z_{k_1}^p \dots Z_{k_r}^p \qquad (n \geq r). \tag{91}$$

The recursion (91) has to be supplemented with the $r-1$ initial conditions $Z_n = a_n$ for $n = 1, \dots, r-1$. This model has two integer parameters, the degree $p \geq 2$ and the number $r \geq 2$ of parts. The recursion (15) defining the 1D model is recovered for $p = r = 2$, whereas the recursion (82) defining Example 3 is recovered for $r = 2$ and p arbitrary.

For physically relevant, i.e., positive initial conditions, the simplest phase diagram one can think of consists of a single critical surface in the space of initial conditions, separating a strong-coupling phase from a weak-coupling one. More complex scenarios allowing for other kinds of behavior in intermediate regimes are however not entirely ruled out.

The strong-coupling phase is captured by the heuristic equation

$$Z_n \sim Z_{n+1-r}^p, \tag{92}$$

generalizing (34) and (83), and yielding an exponentially growing free energy of the form

$$\ln Z_n \approx K\, \mathrm{e}^{n\mu}, \qquad \mu = \frac{\ln p}{r-1}. \tag{93}$$

The weak-coupling phase is captured by the heuristic equation

$$Z_n \sim Z_{n/r}^{pr}, \tag{94}$$

generalizing (46) and (85), and yielding a free energy growing as a power of the sample size modulated by periodic oscillations, of the form

$$\ln Z_n \approx -F(x)\, n^d, \tag{95}$$

where the effective dimension reads

$$d = \frac{\ln pr}{\ln r}, \tag{96}$$

and $F(x)$ is a 1-periodic function of the logarithmic variable

$$x = \frac{\ln n}{\ln r}. \tag{97}$$

The constant K and the function $F(x)$ depend on the $r-1$ initial conditions.

8. Discussion

The stochastic fragmentation model introduced in [31] sparked our interest in revisiting the subject of log-periodic oscillations. The fragmentation model is unique in that it combines the following two characteristics. On the one hand, from a heuristic viewpoint, it can be expected to exhibit some weak discrete scale invariance, in analogy with what occurs e.g. in turbulence or in diffusion-limited aggregation. On the other hand, the numbers $Z_{m,n}$ of jammed configurations obey an exact recursion formula. We have used the latter property to demonstrate by numerical means that the model indeed exhibits the log-periodic oscillations predicted by the former one. To our knowledge, this is the first instance of a statistical-mechanical model where periodic oscillations are reported in the size dependence of a physical quantity.

A 1D analogue of the fragmentation model has then been introduced and investigated in detail. This 1D toy model has many appealing features. First of all, it is simple enough to lend itself to a very detailed investigation. In spite of this, it has a richer behavior than the 2D fragmentation model. There is a critical value a_c of the initial condition, interpreted as a coupling constant, that is somewhat similar to a separatrix in nonlinear dynamics. This critical point separates a strong-coupling phase where the free energy is super-extensive and does not manifest oscillations, from a weak-coupling one where the free energy is extensive and exhibits log-periodic oscillations. The above characteristics can be established on much firmer ground than for the 2D fragmentation model by means of so-called heuristic equations such as (34) and (46). Finally, we have generalized the 1D model into a family of models with two integer parameters, which exhibit essentially the same phenomenology.

This work leaves a number of questions unanswered. The most pressing one concerns what can be established by either rigorous or analytical means about log-periodic oscillations in the fragmentation model. Possible answers range from simply proving their existence to deriving explicit formulas for the log-periodic functions that modulate the bulk configurational entropy and related aspect-ratio-dependent quantities.

Acknowledgments

It is a pleasure to thank Paul Krapivsky for very stimulating exchanges that motivated this work, and for having graciously made available to me the graph shown in Figure 2. A useful discussion with Jérémie Bouttier and Emmanuel Guitter is also acknowledged.

References

[1] G. Jona-Lasinio, The renormalization group: A probabilistic view, Nuovo Cim. B 26 (1975) 99–119.

[2] M. Nauenberg, Scaling representation for critical phenomena, J. Phys. A 8 (1975) 925–928.

[3] T. Niemeijer, J. M. J. van Leeuwen, Renormalization theory for Ising-like spin systems, in: C. Domb, M. S. Green (Eds.), Phase Transitions and Critical Phenomena, Vol. 6, Academic Press, New York, 1976, pp. 425–506.

[4] B. Derrida, J. P. Eckmann, A. Erzan, Renormalisation groups with periodic and aperiodic orbits, J. Phys. A 16 (1983) 893–906.

[5] B. Derrida, L. De Seze, C. Itzykson, Fractal structure of zeros in hierarchical models, J. Stat. Phys. 33 (1983) 559–569.

[6] B. Derrida, C. Itzykson, J. M. Luck, Oscillatory critical amplitudes in hierarchical models, Commun. Math. Phys. 94 (1984) 115–132.

[7] D. Bessis, J. S. Geronimo, P. Moussa, Mellin transforms associated with Julia sets and physical applications, J. Stat. Phys. 34 (1984) 75–110.

[8] C. Itzykson, J. M. Luck, Zeroes of the partition function for statistical models on regular and hierarchical lattices, in: Critical Phenomena (1983 Brasov School Conference), Progress in Physics, Vol. 11, Birkhäuser, Boston, 1985, pp. 45–82.

[9] O. Costin, G. Giacomin, Oscillatory critical amplitudes in hierarchical models and the Harris function of branching processes, J. Stat. Phys. 150 (2013) 471–486.

[10] B. Derrida, G. Giacomin, Log-periodic critical amplitudes: A perturbative approach, J. Stat. Phys. 154 (2014) 286–304.

[11] R. O. Vallejos, C. Anteneodo, Thermodynamical fingerprints of fractal spectra, Phys. Rev. E 58 (1998) 4134–4140.

[12] M. Knežević, D. Knežević, Oscillatory behavior of critical amplitudes of the Gaussian model on a hierarchical structure, Phys. Rev. E 60 (1999) 3396–3398.

[13] J. C. Lessa, R. F. S. Andrade, Log-periodic oscillations for a uniform spin model on a fractal, Phys. Rev. E 62 (2000) 3083–3089.

[14] M. A. Bab, G. Fabricius, E. V. Albano, On the occurrence of oscillatory modulations in the power law behavior of dynamic and kinetic processes in fractals, Europhys. Lett. 81 (2008) 10003.

[15] L. Padilla, H. O. Mártin, J. L. Iguain, Log-periodic modulation in one-dimensional random walks, Europhys. Lett. 85 (2009) 20008.

[16] E. Akkermans, O. Bénichou, G. V. Dunne, A. Teplyaev, R. Voituriez, Spatial log-periodic oscillations of first-passage observables in fractals, Phys. Rev. E 86 (2012) 061125.

[17] G. V. Dunne, Heat kernels and zeta functions on fractals, J. Phys. A 45 (2012) 374016.

[18] J. M. Luck, T. M. Nieuwenhuizen, A soluble quasi-crystalline magnetic model: the XY quantum spin chain, Europhys. Lett. 2 (1986) 257–266.

[19] D. Karevski, L. Turban, Log-periodic corrections to scaling: exact results for aperiodic Ising quantum chains, J. Phys. A 29 (1996) 3461–3470.

[20] R. F. S. Andrade, Detailed characterization of log-periodic oscillations for an aperiodic Ising model, Phys. Rev. E 61 (2000) 7196–7199.

[21] P. Carpena, A. V. Coronado, P. Bernaola-Galván, Thermodynamics of fractal spectra: Cantor sets and quasiperiodic sequences, Phys. Rev. E 61 (2000) 2281–2289.

[22] T. E. Harris, Branching processes, Ann. Math. Statist. 19 (1948) 474–494.

[23] A. M. Odlyzko, Periodic oscillations of coefficients of power series that satisfy functional equations, Adv. Math. 44 (1982) 180–205.

[24] D. Sornette, Discrete-scale invariance and complex dimensions, Phys. Rep. 297 (1998) 239–270.

[25] B. Derrida, H. J. Hilhorst, Singular behavior of certain infinite products of random 2×2 matrices, J. Phys. A 16 (1983) 2641–2654.

[26] C. de Calan, J. M. Luck, T. M. Nieuwenhuizen, D. Petritis, On the distribution of a random variable occurring in 1d disordered systems, J. Phys. A 18 (1985) 501–523.

[27] J. Bernasconi, W. R. Schneider, Diffusion in a one-dimensional lattice with random asymmetric transition rates, J. Phys. A 15 (1982) L729–L734.

[28] J. W. Haus, K. W. Kehr, Diffusion in regular and disordered lattices, Phys. Rep. 150 (1987) 263–406.

[29] T. M. Nieuwenhuizen, J. M. Luck, Singular behavior of the density of states and the Lyapunov coefficient in binary random harmonic chains, J. Stat. Phys. 41 (1985) 745–771.

[30] T. M. Nieuwenhuizen, J. M. Luck, Lifshitz singularities in random harmonic chains: periodic amplitudes near the band edge and near special frequencies, J. Stat. Phys. 48 (1987) 393–424.

[31] E. Ben-Naim, P. L. Krapivsky, Jamming and tiling in fragmentation of rectangles, Phys. Rev. E 100 (2019) 032122.

[32] J. Jäckle, On the glass transition and the residual entropy of glasses, Phil. Mag. 44 (1981) 533–545.

[33] R. G. Palmer, Broken ergodicity, Adv. Phys. 31 (1982) 669–735.

[34] OEIS Foundation Inc., The On-Line Encyclopedia of Integer Sequences (2024).
URL `https://oeis.org`

[35] J. L. Cardy, Finite-Size Scaling, North Holland, Amsterdam, 1988.

[36] V. Privman, Finite Size Scaling and Numerical Simulation of Statistical Systems, World Scientific, Singapore, 1990.